We are IntechOpen,
the world's leading publisher of
Open Access books
Built by scientists, for scientists

6,900
Open access books available

185,000
International authors and editors

200M
Downloads

154
Countries delivered to

Our authors are among the

TOP 1%
most cited scientists

12.2%
Contributors from top 500 universities

CLARIVATE ANALYTICS
BOOK CITATION INDEX
INDEXED

WEB OF SCIENCE™

Selection of our books indexed in the Book Citation Index
in Web of Science™ Core Collection (BKCI)

Interested in publishing with us?
Contact book.department@intechopen.com

Pitting Corrosion Resistance and Inhibition of Lean Austenitic Stainless Steel Alloys

Roland Tolulope Loto

Additional information is available at the end of the chapter

Abstract

The pitting corrosion behavior of 301, 304 and 316 austenitic stainless steels in 2M H_2SO_4 at 0–1.5% NaCl concentrations was investigated through potentiodynamic polarization and optical microscopy analysis. Electrochemical analysis of the pitting corrosion inhibition and surface protection properties of rosemary oil and aniline on the stainless was also performed. The corrosion rate, pitting potential, passivation potential, metastable pitting potential and surface morphology of both steels where significantly altered by changes in chloride concentration, differences in alloy composition and metallurgical properties of the steels. 316 steel had the lowest corrosion rate and highest pitting corrosion resistance followed by 301 steel. The surface morphology of 316 steel was slightly altered at 1.5% NaCl concentration while 301 steel appears to etch with grain boundaries appearing at higher chloride concentration. 304 steel showed no resistance to pitting after 0% NaCl coupled with relatively significant increase in corrosion rate values. Its surface morphology showed the presence of corrosion pits with respect to chloride and inhibitor concentration. Rosemary oil and aniline significantly reduced the corrosion rates values of the stainless steels and with consequent increase in their pitting corrosion resistance; however the compounds had no positive influence on the pitting corrosion behavior of 304 steel.

Keywords: pitting, corrosion, steel, sodium chloride, austenitic

1. Introduction

Lean austenitic stainless steels consisting mainly of 201, 301, 304 and 316 stainless steel alloys have immense applications in food preparation equipment particularly in chloride environments, boat fittings, chemical containers, heat exchangers, marine applications, pharmaceutical industries, petrochemical, offshore drilling, water desalination and diluted acid containers at low temperature, etc., where high strength is of very high importance in the material of

application due to the austenite stability of these alloys which gives a wide range work-hardening rates and ductility [1]. They have less than 20% chromium and 14% nickel content. This category of stainless steels is easily weldable and formable with sufficient corrosion resistance for general purpose applications in mild corrosive environments due to the formation of a passive protective film on the surface of the steels. The passive film consists of the chemical combination of iron and chromium oxy-hydroxide layer, and water containing-compounds at the metal/solution interface [2]. Localized dissolution of the passive film is one of the major causes of pitting corrosion failure of these steels during application. The dissolution tends to be stochastic rather than a visible catastrophic process [3–5].

Previous research on pitting corrosion has shown that it is difficult to experimentally conclude on its mechanism due to its random nature and breakdown of the steel's passive film is due to the selective dissolution of the iron substrate metal [6–12]. The electrochemical process of pitting corrosion results in the formation of microscopic holes of various sizes on metal surfaces which tends to rapidly increase in dimension especially in the presence of chloride ions within the corrosive medium. Under appropriate conditions lean austenitic stainless steels pits at different rates due to differences in chromium, nickel content and metallurgical structure. Due to its localized nature pitting corrosion may be undetected at the onset as only microscopic regions of stainless steel surfaces corrodes while the remaining portion remains passive and cathodic. Pitting is particularly insidious in nature due to the extent of rapidly penetrating into the mass of the metal. The result of such rapid perforations can induce leakage of fluid or alternatively, pitting to crack transition may occur with consequential crack nucleation and growth which leads to brittleness and catastrophic failure. In most cases the corrosive damage is in its advanced stages before detection. The need to further understanding the pitting corrosion mechanism and the influence of organic chemical inhibitors on the electrochemical process resulting in pitting is of very high importance.

1.1. Pitting corrosion mechanism in the presence of chlorides

Pitting corrosion mechanism generally consists of pit initiation and pit propagation stages during the metal dissolution process. The pit initiation stage is the product of the electrochemical action of aggressive ions such as chlorides, sulfates, thiosulfates, etc., at specific regions, sites or flaws in the oxide layer which in some cases causes segregation of alloy elements on the metallic surface. Once a pit nucleates, pit propagation proceeds autocatalytically. The autocatalytic reaction produces cavities initiated at the surface, resulting in a myriad of shapes and sizes. This however depends on the microstructure of the material, electrolyte and various electrochemical factors. Chlorides are most commonly responsible for pit formation on stainless steels as shown in **Figure 1** according to Eqs. (1)–(10). They locally disrupt the passive oxide film at preferential sites especially sites consisting of sulfide inclusions resulting in the gradual formation of corrosion pits. The passive film of stainless steels is made up of adsorbed oxygen. In the presence of chloride ions the higher affinity of oxygen allows for displacement of chloride ions, however as the alloy potential becomes more positive and chloride ions displaces the oxygen atoms and diffuse to the metal/oxide layer [13–20]. The chloride ion diffusion is due to electrostatic attraction. The presence of chloride ions within corrosion pits
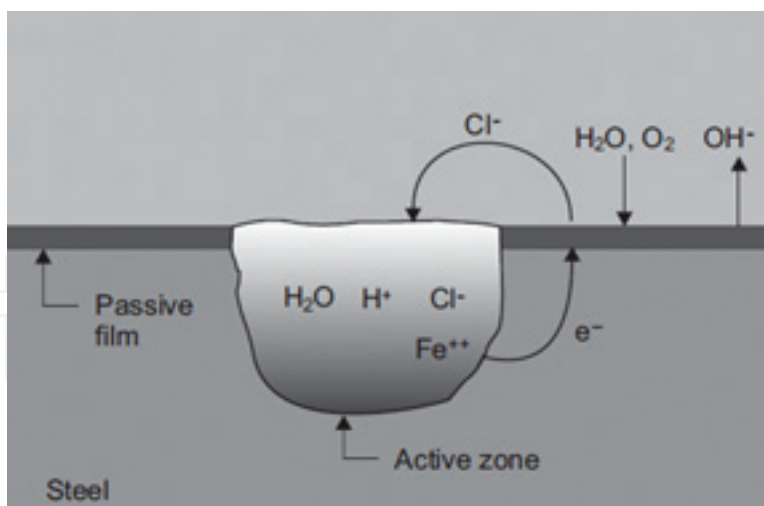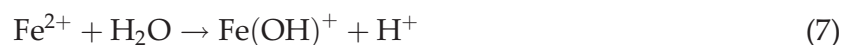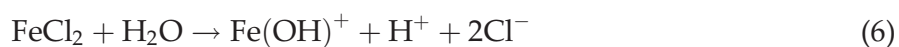
Figure 1. Chloride attack on stainless steel alloy.

stimulates the redox electrochemical reactions necessary for the propagation of the pits. This phenomenon increases the entropy of the reaction species within the pit thus accelerating the localized corrosion of stainless steels. Changes in the electrolyte occurs due to high anodic dissolution rates, and limited diffusion of ionic species The increase in acidity of the electrolyte within the pit caused by insufficient oxygen further accelerates the pitting corrosion reactions in addition to the significant difference between the anode and cathode areas of the steel. This results in metal dissolution leading to cation production within the pits. Pit initiation also occurs due to intermetallic inclusions, micro-segregations, stress points and regions due to dislocations and fatigue.

Anodic reactions inside the pit:

$$3Fe + 4H_2O \rightarrow Fe_3O_4 + 8H^+ + 8e \tag{1}$$

$$Fe \rightarrow Fe^{2+} + 2e^- \text{(dissolution of iron)} \tag{2}$$

$$Fe^{2+} + H_2O \rightarrow Fe(OH)^+ + H^+ \tag{3}$$

$$3Fe(OH)^+ + H_2O \rightarrow Fe_3O_4 + 5H^+ + 2e \tag{4}$$

In the presence of Cl^-, the hydrolysis of Fe^{2+} is accelerated, as shown in the reactions below;

$$Fe^{2+} + Cl^{2-} \rightarrow FeCl_2 \tag{5}$$

$$FeCl_2 + H_2O \rightarrow Fe(OH)^+ + H^+ + 2Cl^- \tag{6}$$

$$Fe^{2+} + H_2O \rightarrow Fe(OH)^+ + H^+ \tag{7}$$

The electrons given up by the anode flow to the cathode (passivated surface) where they are discharged in the cathodic reaction:

$$\tfrac{1}{2}O_2 + H_2O + 2e^- \leftrightarrow 2(OH^-) \tag{8}$$

$$H^+ + e \rightarrow H \tag{9}$$

$$2H^+ + 2e \rightarrow H_2 \tag{10}$$

Pit propagation involves consistent anodic dissolution by diffusion due to high concentration of metallic and chloride ions within corrosion pits, hence a high concentration of hydrogen ions due to hydrolysis [21]. The corrosion process within the pit is a specific type of anodic reaction whose conditions enables and is necessary for electrochemical reactions within the pit. The diffusion of metallic cations to the pit exterior causes the chloride concentration within the pit to increase resulting in accelerated propagation of the pitting corrosion already taking place. A high cation concentration already exists within the propagating pit, and more chloride ions diffuse into the pit to maintain solution concentration [22, 23]. This phenomenon prevents the repassivation of the stainless steel alloy which otherwise will hinder the pit propagation mechanism.

1.2. Metastable pitting

Repassivation of the oxide protective film on stainless steels causes newly formed pits to disappear for several reasons. Metastable pits are visible during potential scanning indicated by the current fluctuations at very low potentials, below the values necessary for stable pits to occur [24–26]. The pits are microscopic in dimension with a very short lifespan resulting smaller damages on the metallic surface. The passive film on stainless steels is locally damaged during the metastable pitting process before metal dissolution and then surface repassivation. At low potentials, dissolution cannot continue but as the potential of the system increases, the anodic dissolution rate increases and the peak current and lifetime of the metastable pit increase before repassivation. The lower the potential at which stainless steels repassivate after metastable pit formation, the higher the pitting corrosion resistance of the steel. The size of inclusions, flaws, and impurities as well as the presence of fatigue stress are important parameters for the occurrence and properties of metastable pits [27]. There is consistency and correlation between the behavior of stable and metastable pitting. If the acidity and concentration of aggressive ions necessary to keep dissolution in a pit cannot be maintained, repassivation would happen. When a pit has developed to the critical condition which can maintain continuous dissolution in the pit, the metastable pit would transform to a stable pit. The two major criteria responsible for metastable pitting are chloride ion concentration and effect of alloying elements. Chloride in the early stage of pitting corrosion would damage the passive film, and promote the nucleation of metastable pits. The larger the chloride concentration, the higher the metastable pitting nucleation rate. Therefore, with the increase of chloride concentration, both the nucleation and the growth of metastable pits are promoted. According to Burstein [28, 29], this is directly associated with the observation that the number of surface sites available for development of a metastable pit decreased with decreasing chloride for all potentials. A number of researchers studied the effect of alloying elements on the formation of metastable pitting and observed that stainless steel alloys with varying concentration of chromium and molybdenum experience a decrease in the number of metastable events with time due to

improve corrosion resistance of the passive film resulting in decrease in available initiation sites [30–33].

2. Potentiodynamic polarization study and inhibition of the pitting corrosion of 301, 304 and 316 in acid chloride media

Pitting corrosion initiation and propagation is subject to factors responsible for any electro-chemical corrosion reaction such as charge-transfer mechanisms, ohmic effects and mass transport phenomena. The importance of environmental and material factors relevant to the pitting process, such as electrochemical potential, alloy composition, electrolyte concentration and temperature can be understood by their role on pit growth stability. Influence of the passive film characteristics and the mechanism of the initiation of pitting or breakdown of the otherwise protective passive film are highly important in the study of pitting corrosion. Studies performed on metastable and stable pit growth of metallic alloys have seen consider-able progress on propagation processes, conditions and effects of electrochemical variables. Several mechanisms have been proposed to explain the passivity breakdown. Compounds capable of releasing chloride ions to aqueous environments have strong possibility of causing pitting corrosion failure in stainless steels. The chloride ion is highly electronegative and very reactive with specific compounds and elements. The polarization behavior in chloride ion-containing solution has been investigated for decades and a number of conclusions on its electrochemical influence on the pitting corrosion mechanism have been reached [34–41]. In this chapter, the pitting corrosion resistance of type 301, 304 and 316 austenitic stainless steels exposed to 2 M H_2SO_4 acid at specific chloride concentrations will be discussed with focus on the potentiodynamic polarization behavior of the steels, characterization of the pitting suscep-tibility of the steels in the environments under study, metastable pitting, influence of chloride ion concentration and inhibitor protection through the use of rosemary oil and aniline.

2.1. Experimental methods

2.1.1. Materials and preparation

301, 304, 316 austenitic stainless steels (301SS, 304SS and 316SS) sourced commercially had a nominal composition (wt.%) as shown in **Table 1**. The steel samples machined and afterwards grinded with silicon carbide abrasive papers (80, 120, 220, 320, 600, 800 and 1000 grits) before cleansing with deionized water and acetone for potentiodynamic polarization tests according to ASTM G1–03 [42]. Polarization measurements were conducted out at ambient temperature of 30°C using a three electrode system and glass cell containing 200 mL of the corrosive test solution with Digi-Ivy 2311 potentiostat. 301SS, 304SS, 316SS electrodes mounted in acrylic resin with an exposed surface area of 0.6, 0.79 and 1.33 cm^2 were prepared according to ASTM G59–97 [43]. The polarization plots were obtained at a scan rate of 0.0015 V/s between poten-tials of −0.5 and +1 V according to ASTM G102–89 [44]. A platinum rod was used as the counter electrode and a silver chloride electrode (Ag/AgCl) as the reference electrode. Corro-sion current density (J_{corr}) and corrosion potential (E_{corr}) values were obtained using the Tafel

Element symbol	Si	N	Ni	Mo	Cr	Mn	P	S	C	Fe
% Composition (301SS)	1	0.1	8	–	16	2	0.045	–	0.15	72.7
% Composition (304SS)	0.75	0.1	8	–	18	2	0.045	0.03	0.03	69.31
% Composition (316SS)	0.75	0.1	11	3	18	2	0.045	0.03	0.08	65

Table 1. Percentage nominal composition (wt.%) of 301SS, 304SS and 316SS.

extrapolation method. The corrosion rate (γ) and the inhibition efficiency (η_2, %) were calculated from the mathematical relationship:

$$C_R = \frac{0.00327 \times J_{corr} \times E_{qv}}{D} \quad (11)$$

where J_{corr} is the current density in A/cm^2, D is the density in g/cm^3 and E_{qv} is the sample equivalent weight in grams. 0.00327 is a constant for corrosion rate calculation in mm/y [45]. 2MH$_2$SO$_4$/0.25, 0.5, 0.75, 1, 1.25 and 1.5% NaCl solution, prepared from analar grade of H$_2$SO$_4$ acid (98%) and recrystallized NaCl with deionized water. *Rosmarinus officinalis* obtained from NOW Foods, USA is a golden, translucent, oily liquid with a molar mass (active groups) of 691.14 g/mol. Aniline obtained from has a molar mass of 81.38 g/mol. It is a dark translucent liquid soluble in water with a molar mass of 93.13 g/mol. The compounds were prepared in volumetric concentrations of 5% in 200 mL of 2MH$_2$SO$_4$/0.25% and 1.5% NaCl solution. Optical images of steel samples before and after corrosion were analyzed with Omax trinocular metallurgical through the aid of ToupCam analytical software.

2.2. Result and discussion

2.2.1. Potentiodynamic polarization studies

The corrosion polarization behavior of 301SS, 304SS and 316SS samples in 2 M H$_2$SO$_4$ at 0–1.5% NaCl is shown in **Figures 2–4**. **Table 2** shows the results for the potentiodynamic polarization curves. 316SS generally showed a higher resistance to corrosion than 301SS and 304SS at 0–1.5% NaCl from observation of corrosion rate values in **Table 2**, however its corrosion resistance is subject to changes in chloride ion concentration in the acid solution. The corrosion rates of 304SS were relatively higher than 316SS and 301SS. The surface of 304SS tends to more easily form soft acid, compared to the other steels from the concept Lewis acid–base theory, thus adsorbing chloride and sulfate ions which accelerates its corrosion rate faster than the others [46]. The corrosion rate of 301SS is comparable to 304SS from 0 to 0.5% NaCl having generally similar values but its corrosion rate remained constant after 0.5% due to its more stable electrochemical corrosion resistance behavior to changes in higher chloride ion concentration.

The corrosion rate values of the 301SS, 304SS and 316SS studied corresponds with values of corrosion current and polarization resistance. The cathodic and anodic Tafel slopes for 301SS and 304SS were generally constant with minor variation due to consistent redox electrochemical reactions of hydrogen evolution, oxygen reduction and oxidation reactions taking place at
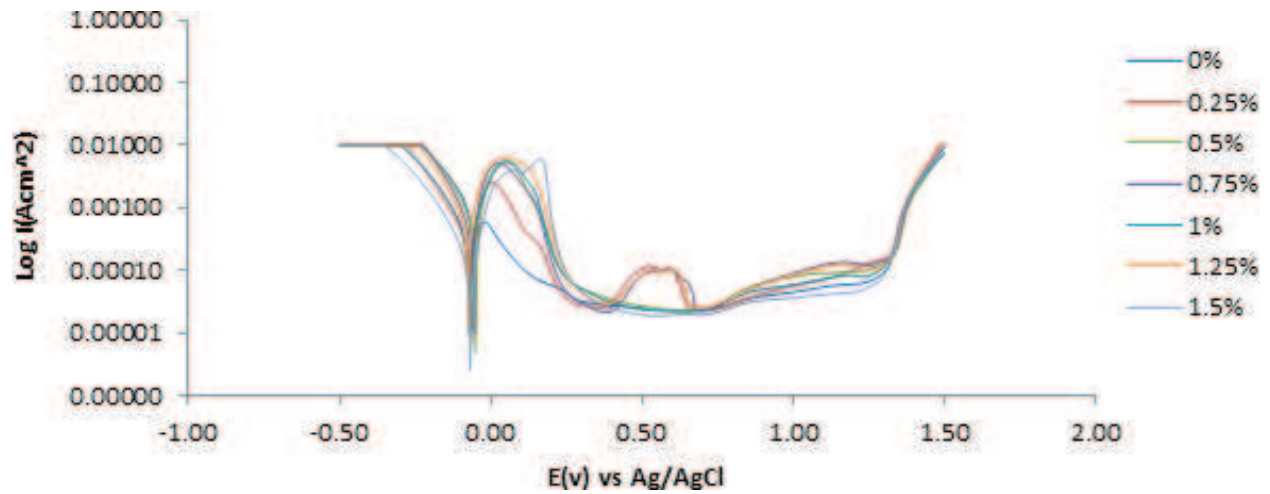
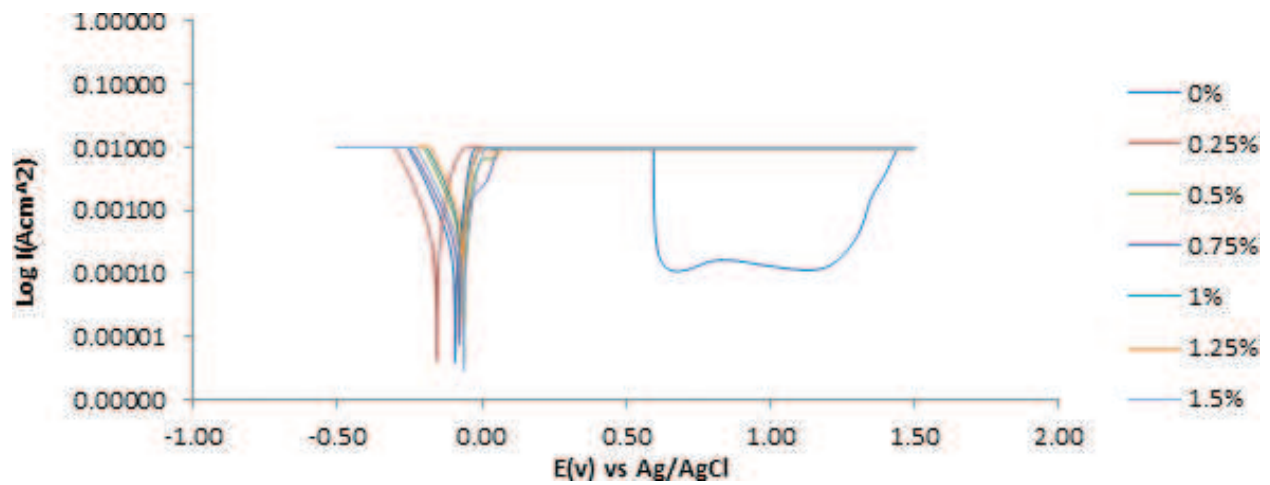**Figure 2.** Potentiodynamic polarization curves of 301SS in 2 M H_2SO_4/0–1.5% NaCl.

Figure 3. Potentiodynamic polarization curves of 304SS in 2 M H_2SO_4/0–1.5% NaCl.
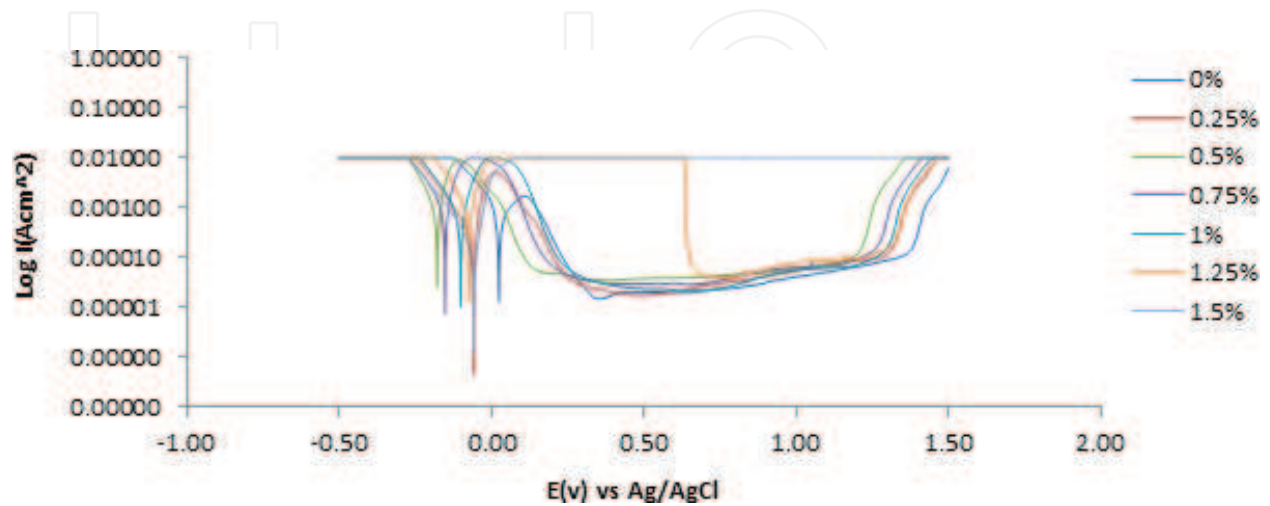
Figure 4. Potentiodynamic polarization curves of 316SS in 2 M H_2SO_4/0–1.5% NaCl.

Sample	2 M H$_2$SO$_4$/NaCl conc. (%)	Corrosion rate (mm/y)	Corrosion current (A)	Corrosion current density (A/cm^2)	Corrosion potential (V)	Polarization resistance, R_p (Ω)	Cathodic Tafel slope, B_c (V/dec)	Anodic Tafel slope, B_a (V/dec)
301SS								
A	0	9.086	5.23E-04	8.72E-04	−0.052	31.23	−6.674	3.527
B	0.25	14.889	8.57E-04	1.43E-03	−0.064	16.17	−8.304	3.420
C	0.5	16.314	9.39E-04	1.57E-03	−0.051	14.37	−7.676	3.231
D	0.75	14.681	8.45E-04	1.41E-03	−0.062	19.37	−8.498	3.600
E	1	14.976	8.62E-04	1.44E-03	−0.071	17.39	−7.692	3.513
F	1.25	15.306	8.81E-04	1.47E-03	−0.074	19.17	−8.151	3.620
G	1.5	15.584	8.97E-04	1.50E-03	−0.068	13.11	−8.497	3.030
304SS								
A	0	7.694	5.92E-04	7.49E-04	−0.092	53.57	−10.89	5.289
B	0.25	16.766	1.29E-03	1.63E-03	−0.06	91.83	−11.117	5.433
C	0.5	18.066	1.39E-03	1.76E-03	−0.062	42.35	−10.49	5.146
D	0.75	21.315	1.64E-03	2.08E-03	−0.081	49.01	−10.08	5.127
E	1	22.875	1.76E-03	2.23E-03	−0.073	13.74	−9.026	4.432
F	1.25	26.774	2.06E-03	2.61E-03	−0.067	9.77	−9.853	4.245
G	1.5	30.543	2.35E-03	2.97E-03	−0.062	7.42	−10.91	4.121
316SS								
A	0	1.176	1.50E-04	1.13E-04	0.024	23.34	−6.971	2.486
B	0.25	2.249	2.87E-04	2.16E-04	−0.06	40.34	−8.721	−0.925
C	0.5	3.197	4.08E-04	3.07E-04	−0.178	12.37	−9.826	−1.123
D	0.75	3.879	4.95E-04	3.72E-04	−0.153	13.49	−8.203	2.725
E	1	5.337	6.81E-04	5.12E-04	−0.102	13.92	−8.581	6.976
F	1.25	6.403	8.17E-04	6.14E-04	−0.075	14.49	−8.585	2.033
G	1.5	7.273	9.28E-04	6.98E-04	−0.058	18.29	−8.691	5.979

Table 2. Potentiodynamic polarization results for 301SS, 304SS and 316SS in 2 M H$_2$SO$_4$/0–1.5% NaCl.

the steel surfaces with respect to chloride concentration. The observed variation in anodic Tafel slope for 316SS compared to its cathodic Tafel slope with respect to chloride concentration is probably due to the slow electron transfer step resulting from changes in rate controlling step, influence of potential controlled conditions and the presence of molybdenum in its metallurgical structure [47, 48]. This observation corresponds with significant changes in corrosion potential of 316SS compared to 310SS and 304SS. The corrosion potential transits to positive potentials after 0.25% NaCl due to release of fewer electrons which increases the anodic reaction mechanism. The anodic-cathodic polarization scans for 301SS and 304SS (**Figures 2** and **3**) were quite similar at all NaCl concentrations compared to 316SS (**Figure 4**) which showed as a wide scatter over the potential domain. This observation shows that

changes in NaCl concentration have limited influence on the polarization behavior and redox corrosion reaction mechanisms of 301SS and 304SS as stated earlier from evaluation of anodic and cathodic Tafel slopes.

2.2.2. Pitting corrosion evaluation

Study of the pitting corrosion resistance of 301SS, 304SS and 316SS was done through evaluation of pitting, passivation and metastable pitting potentials, and their passivation range. Theoretically the pitting potential is the potential at which pitting corrosion occurs, but below which pits do not nucleate. The passivation potential is the potential value at which potentials greater to or equal to this potential, pit do propagate, but below which the metal retains its passivity. The stainless steel samples exhibited unique pitting corrosion resistance characteristics that differ significantly from each other. 316SS showed the highest resistance to pitting corrosion from observation of potentiostatic values in **Table 3** at 0–1.25% NaCl. At 1.5% NaCl concentration 316SS showed no pitting corrosion resistance behavior from observation of **Figure 3**, as a result the steel failed immediately after anodic polarization. The passivation range of 316SS which shows the extent to which stainless steels sustains their passive film remain unchanged at 0.25% NaCl, after which it increased at 0.5% NaCl and remained

Sample	2 M H_2SO_4/NaCl conc. (%)	Metastable pitting potential (V), E_{mpitt}	Passivation potential (V), E_{pass}	Pitting potential (V), E_{pitt}	Passivation range (V)
310SS					
A	0	−0.07	0.12	1.23	1.11
B	0.25	−0.02	0.23	1.27	1.04
C	0.5	0.01	0.23	1.30	1.07
D	0.75	0.00	0.24	1.29	1.05
E	1	0.02	0.26	1.24	0.98
F	1.25	0.05	0.26	1.24	0.98
G	1.5	0.13	0.28	1.24	0.96
304SS					
A	0	0.55	0.62	1.18	0.56
316SS					
A	0	0.08	0.32	1.33	1.01
B	0.25	−0.02	0.24	1.25	1.01
C	0.5	−0.13	0.13	1.16	1.03
D	0.75	−0.07	0.17	1.20	1.03
E	1	0.00	0.23	1.26	1.03
F	1.25	0.58	0.66	1.29	0.63
G	1.5	0.00	0	0	0

Table 3. Potentiostatic results of pitting passivation and metastable potentials for 301SS, 304SS and 316SS in 2 M H_2SO_4/ 0–1.5% NaCl solution.

constant till 1.25% NaCl at 0.63 V. This observation shows that at a particular chloride concentration 316SS instantaneously loses it passivity. In the presence of chlorides, the pitting potential of 316SS decreased with respect to concentration and remained at values below the pitting potential of the control sample (0% NaCl) due to the action of chloride ions in destroying the passivity of the steel. At 0% NaCl, 316SS passivated at 0.32 V, on addition of chlorides, the steel passivated at lower potentials until 1.25% where it passivated at significantly higher potentials. The phenomenon attests to the prevailing characteristics of the steel in chloride containing environments. A corresponding observation was noted for metastable potential values. Increase in chloride concentration caused a significant rise in the metastable region of the polarization curves of 301SS and 316SS, an indication that the passive film is undergoing localized but transient pitting due to temporary breakdown of the passive film, and the creation and growth of small, occluded cavities before stable passivation. These events are determined by the steels composition and strength of the passive film.

301SS showed generally uniform but narrower passivation behavior over the potentiostatic domain at specific chloride concentrations and retained its passivation behavior at 1.5% NaCl in comparison to 316SS. The passivation range of 310SS decreased after 0% NaCl due to the action of chlorides on the steel, hence its passive protective film reduced in strength compared to 316SS, however the pitting potential values of 301SS increased till 0.75% NaCl before decreasing to values higher than 0% NaCl concentration. This observation do not mean 301SS is more resistant to pitting corrosion than 316SS because in the presence of chlorides 301SS passivates at higher potentials compared to 316SS which passivates at lower potentials hence 316SS has a wider passivation range than 301SS, signifying a more resistance passive film to pitting corrosion. Despite these observations 301SS has better metastable pitting resistance than 316SS as transient pits appears for the steel at higher potentials compared to 316SS. 304SS displayed no pitting corrosion resistance after 0% NaCl concentration. The weak resistance of 304SS is due to excessive adsorption through diffusion of chloride ions at the metal-film interface which induces the electrolytic transport of metallic cations to the acid/chloride solution.

Elemental composition and metallurgical structure are the major factors responsible for the differences in electrochemical behavior and passivation characteristics the three stainless steels studied. Observation of **Table 1** shows that steels have the same elemental composition consisting of an austenite microstructure stabilized by their nickel content, but with the exception of Mo in 316SS. Molybdenum is an important alloy element widely used in metallurgy and has been known to improve the corrosion resistance of stainless steel alloys, being a ferrite former in the presence of manganese and nickel. In the acid/chloride solution it enriches Cr at the metal/solution interface which stabilizes and thickens the passive film [49–57].

2.2.3. Pitting corrosion inhibition

Alloying elements have strong influence on the electrochemical behavior and pitting corrosion resistance of stainless steels. Nickel, chromium, molybdenum and in some cases, titanium, nitrogen, manganese, vanadium are responsible for the properties and strength of the passive film formed on stainless steels [58–60]. Chromium content is one of the major criteria in

categorizing austenitic stainless steels and has been observed to significantly change the potentiostatic parameters used in studying pitting corrosion resistance of stainless steels [61, 62]. Sufficient nickel within the iron matrix improves stainless steel resistance to pitting as it stabilizes the austenite phase and limits the ferrite content which if too high may result in lower rust resistance and ductility. Pitting corrosion can also be prevented in many cases with similar methods used to control general corrosion. The most common method of which is the use of chemical compounds to modify the environment during application [63–67]. Studies have shown that inhibitor adsorption on metallic surface depends on the physicochemical characteristics of inhibitor molecule such as functional groups, steric factors, aromaticity, electron density of the donor atoms, π-orbital character of donating electrons, polymerization resulting in formation of protective film and the electronic structure of the molecules [68, 69]. Most of the well-known corrosion inhibitors are organic compounds containing functional groups of heteroatoms capable of chemically reacting through adsorption with valence electrons of stainless steel surfaces at the metal solution interface [70, 71].

In line with the current trend on corrosion inhibition, two known corrosion inhibiting compounds previously used for general corrosion inhibition of carbon steels was used to assess their pitting corrosion potential of the 301SS, 304SS and 316SS under study (ROSO and ANL) [72–74]. The potentiodynamic curve resulting from the use of ROSO compound on 301SS, 304SS and 316SS, and ANL compound on 304SS is shown in **Figure 5**. In the presence of ROSO, the corrosion current densities of 316SS, 304SS and 301SS were significantly influenced, as a result the general corrosion rates of the steel samples at 0.25 and 1.5% NaCl (**Table 4**) reduced drastically due to the electrochemical action of the ROSO molecules in the acid chloride solution. The electrolytic diffusion of chloride and sulfate ions were effectively hindered by the interaction of ROSO molecules with the steel surfaces, which in effect hindered the release of metal cations resulting from anodic oxidation. 316SS had the lowest corrosion rates followed by 301SS. The corrosion potential of 301SS, 304SS and 316SS in the presence of ROSO shifted to negative potentials signifying the dominant cathodic inhibiting property of ROSO [75, 76]. Changes in the cathodic and anodic Tafel slopes were quite similar for 316SS
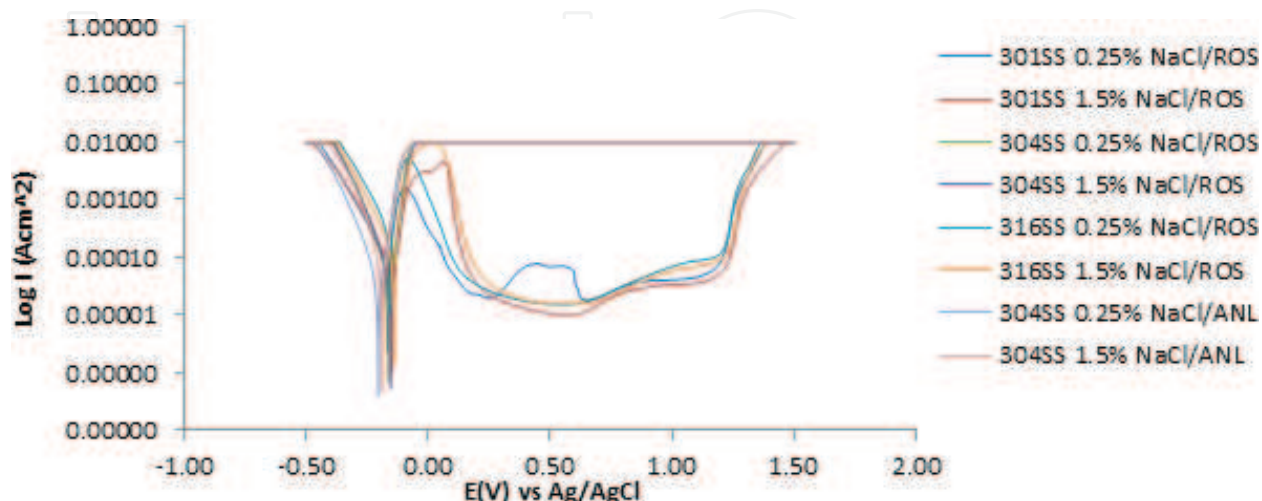

Figure 5. Potentiodynamic polarization curves of 301SS, 304SS and 316SS in 2 M H_2SO_4/5% ROSO at 0.25 and 1.5% NaCl.

Sample	2 M H$_2$SO$_4$/NaCl conc. (%)	Corrosion rate (mm/y)	Corrosion current (A)	Corrosion current density (A/cm^2)	Corrosion potential (V)	Polarization resistance, R_p (Ω)	Cathodic Tafel slope, B_c (V/dec)	Anodic Tafel slope, B_a (V/dec)
ROSO								
301SS	0.25	2.552	1.93E−04	2.45E−04	−0.165	154.67	−8.416	5.107
301SS	1.5	2.684	2.03E−04	2.57E−04	−0.148	140.53	−8.407	5.012
304SS	0.25	8.817	5.15E−04	8.59E−04	−0.161	653.39	−11.790	10.910
304SS	1.5	5.490	3.21E−04	5.35E−04	−0.152	409.85	−11.010	9.230
316SS	0.25	0.234	2.98E−05	2.24E−05	−0.157	1527.33	−7.822	5.604
316SS	1.5	0.565	7.21E−05	5.42E−05	−0.141	1078.19	−8.752	6.950
ANL								
304SS	0.25	0.852	6.56E−05	8.30E−05	−0.204	392.00	−10.710	25.510
304SS	1.5	1.604	1.23E−04	1.56E−04	−0.190	208.20	−11.700	22.470

Table 4. Potentiodynamic polarization results for 301SS, 304SS and 316SS in 2 M H$_2$SO$_4$/5% ROSO at 0.25% and 1.5% NaCl.

Sample	2 M H$_2$SO$_4$/NaCl Conc. (%)	Metastable pitting potential (V), E_{mpitt}	Passivation potential (V), E_{pass}	Pitting potential (V), E_{pitt}	Passivation range (V)
301SS	0.25%	−0.12	0.13	1.17	1.04
301SS	1.5%	0.03	0.15	1.20	1.05
316SS	0.25%	−0.10	0.11	1.14	1.03
316SS	1.5%	−0.02	0.2	1.20	1.00

Table 5. Potentiostatic results of pitting passivation and metastable potentials for 301SS, 304SS and 316SS in 2 M H$_2$SO$_4$/5% ROSO at 0.25 and 1.5% NaCl.

and 301SS, but contrast the values obtained for 304SS due to the higher degree of corrosion reactions taking place on 304SS surface. Observation of the potentiostatic data of the three steel samples in **Table 5** showed some mild changes in their values. 316SS at 0.25% NaCl passivated at lower potential of 0.11 V following metastable pitting activity to pit at 1.14 V resulting in a passivation range of 1.03 V while at 1.5% NaCl concentration, pitting corrosion resistance was displayed on the polarization curves resulting in a passivation range of 1.00 V compared to the curve without ROSO compound (**Table 4**, **Figure 4**) where no resistance to pitting corrosion was observed. 301SS passivated at lower potentials following metastable pitting and pitted at higher potentials at 0.25 and 1.5% NaCl concentration resulting in a slightly higher passivation range, thus higher pitting corrosion resistance. ROSO compound had no significant electro-chemical influence of the pitting corrosion activity of 304SS despite improved general corrosion resistance. This confirms the earlier statement that metallurgical properties of stainless steel alloys have significant influence on their pitting corrosion resistance. This observation informed the use of ANL compound on 304SS. The corrosion rates of 304SS in the presence of ANL compound significantly decrease further than values obtained in the presence of ROSO

compound; however there was no noticeable change in the potentiodynamic polarization curve depicting resistance to pitting corrosion though fewer pits were observed on the steel from optical microscopy analysis which will be discussed later. The observations so far show 304SS has very weak resistance to the electrochemical action of chloride ions. Without chloride 304 displayed limited resistance to pitting corrosion as shown in (**Table 3**, **Figure 3**).

2.2.4. Thermodynamics of corrosion inhibition

The adsorption strength of ROSO on 301SS, 304SS and 316SS, and ANL on 304SS was calculated from the thermodynamics of the corrosion inhibition mechanism. Calculated results of Gibbs free energy (ΔG_{ads}°) for the adsorption process is shown in **Table 6**, and evaluated from the mathematical relationship below [77]:

$$\Delta G_{ads}^{\circ} = -2.303RT log[55.5K_{ads}] \tag{12}$$

where 55.5 is the molar concentration of water in the solution, R is the universal gas constant, T is the absolute temperature and K_{ads} is the equilibrium constant of adsorption. K_{ads} is related to surface coverage (θ) from the Langmuir equation. The presence of impurities, flaws, etc., on studied stainless steel surfaces has a strong influence on results obtained for ΔG_{ads}° [78]. The amount of oxidized metal cations passed into the corrosive media is directly related to the extent of coverage of ROSO and ANL compound. Negative ΔG_{ads}° results show the spontaneity and stability of the adsorption mechanism. Values of ΔG_{ads}° around −20 kJ/mol shows physisorption adsorption reaction while values around −40 kJ/mol or higher involve charge sharing or chemisorption due to chemical interaction among the reacting species [79]. The ΔG_{ads}° values obtained for ROSO and ANL interaction on the 301SS, 304SS and 316SS shows chemisorption adsorption of ROSO and ANL molecules on the steel surfaces in response to competitive adsorption of chloride and sulfate ions.

Specimen	NaCl concentration (%)	Surface coverage (θ)	Equilibrium constant of adsorption (K)	Gibbs free energy, ΔG (kjmol^{-1})
ROSO				
301SS	0.25	0.829	66825.7	−37.48
301SS	1.5	0.828	66439.8	−37.47
304SS	0.25	0.474	12463.8	−33.32
304SS	1.5	0.820	63082.0	−37.34
316SS	0.25	0.896	119302.8	−38.92
316SS	1.5	0.922	164090.6	−39.71
ANL				
304SS	0.25	0.949	34792.7	−35.87
304SS	1.5	0.947	33608.3	−35.78

Table 6. Data for Gibbs free energy (ΔG_{ads}°), surface coverage (θ) and equilibrium constant of adsorption (K_{ads}) for ROSO and ANL adsorption on 301SS, 304SS and 316SS.

2.2.5. Optical microscopy analysis of 301SS, 304SS and 316SS morphology

The optical microscopy images of 301SS, 304SS and 316SS before corrosion and after the corrosion test at 0, 0.25 and 1.5% NaCl are shown from **Figures 6(a)–8(c)** at mag. 40×. **Figure 9 (a)–Figure 11(b)** shows the images of 301SS, 304SS and 316SS after corrosion in the presence of ROSO compound while **Figure 11**(**a**, **b**) shows the images of 304SS after corrosion in the presence of ANL compound. Severe morphological deterioration is clearly visible on 304SS (**Figure 7(a–d)**) due to the action of chloride and sulfate ions. At 0% NaCl (**Figure 7(b)**) the serrated edges and lines on the steel surface are faintly visible due to corrosion. Significant number of corrosion pits can be observed due to surface oxidation and release of metal cations into the solution, though sulfate ions is solely responsible for these observations, however at 0.25% NaCl (**Figure 7(c)**) the number of corrosion pits have increased significantly and they appear to be deeper due to the action of chloride ions. The corrosion pits in **Figure 7(d)** appear to be smaller, while the surface morphology seems rougher then the image in **Figure 7(c)**. Results from potentiodynamic study shows the highest corrosion rate for 304SS at 1.5% NaCl, thus it is suggested that the presence of excessive chloride ions in solution does not necessarily
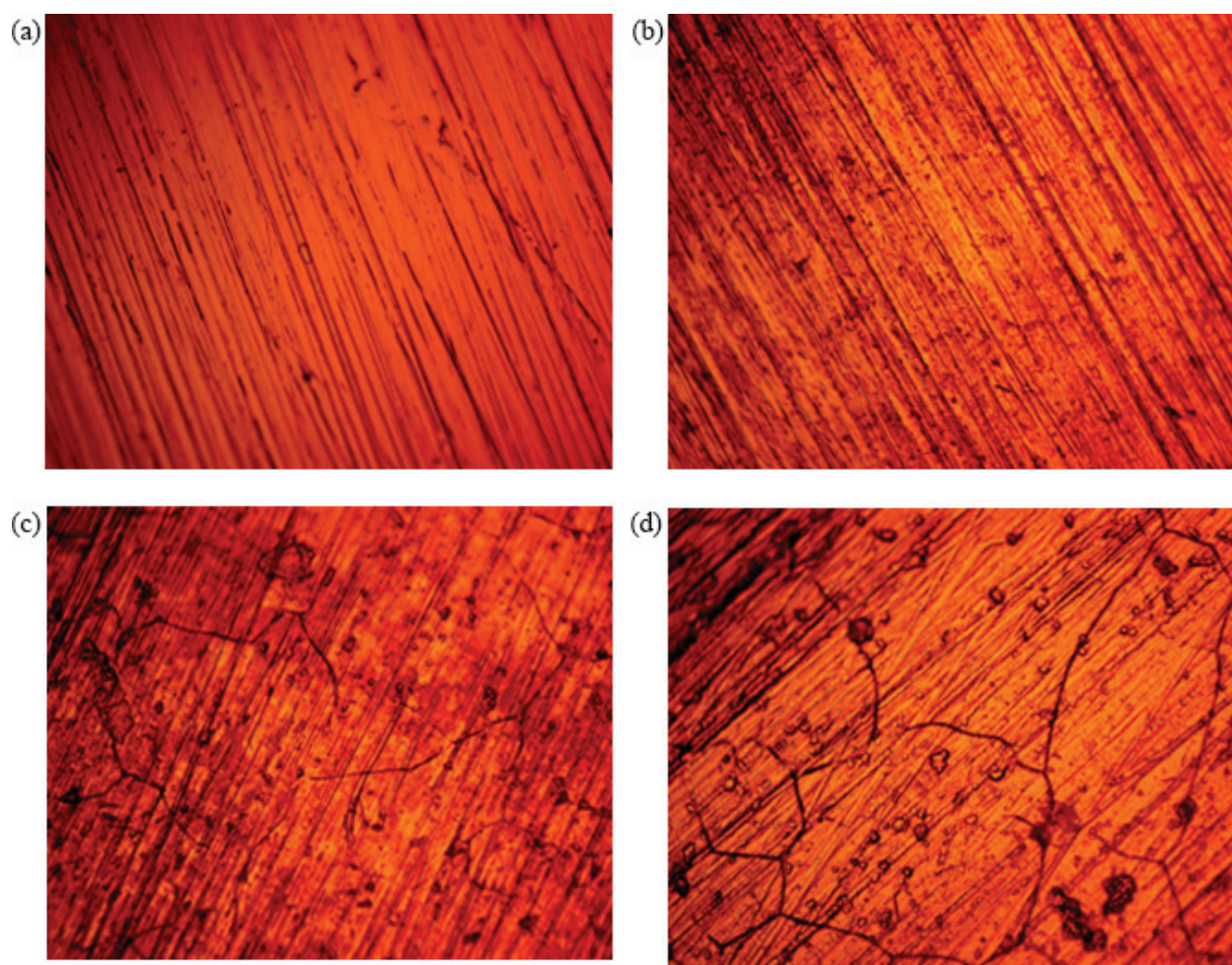

Figure 6. Optical microscopy image 301SS at mag. 40× (a) before corrosion, (b) at 0% NaCl, (c) at 0.25% NaCl and (d) at 1.5% NaCl.
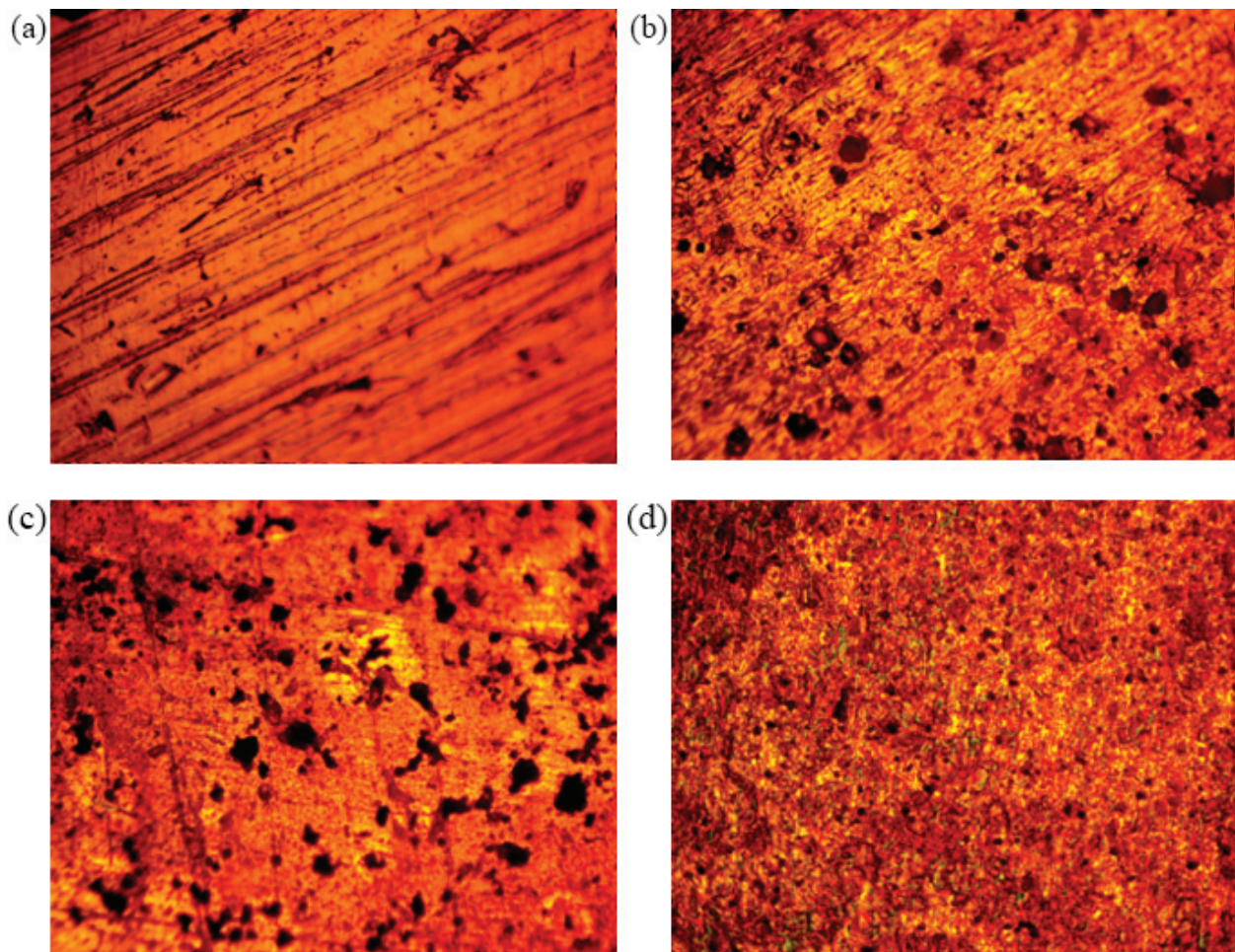
Figure 7. Optical microscopy image 304SS at mag. 40× (a) before corrosion, (b) at 0% NaCl, (c) at 0.25% NaCl and (d) at 1.5% NaCl.

mean more corrosion pits even though the general corrosion rate may be higher. There seems to be a threshold level of chloride concentration responsible for the size of corrosion pits.

Corrosion pits are clearly absent from 301SS (**Figure 7(b–d)**) due to the resilience of its passive film. What appears on its morphology (**Figure 7(c)**) seems to be shallow indentations and faint appearance of the grain boundaries due to mild etching by the chloride ions. **Figure 7(d)** shows a worn-out morphology compared to **Figure 7(c)** with the indentation larger and the grain boundary much more visible. In general, the morphology of 301SS shows a highly resistant steel to pitting. The morphology of 316SS remained unchanged or probably etched at 0% NaCl (**Figure 8(b)**). In 0.25% NaCl, (**Figure 8(c)**) the surface morphology seems to have worn out compared to **Figure 8(b)**. These observations show the electrochemical action of chlorides and sulfates have limited influence on the pitting corrosion resistance of 316SS. At 1.5% NaCl (**Figure 8(d)**), significantly morphological deterioration occurred; the grain boundaries are also faintly visible with numerous micro indentations. The morphologies of 301SS and 316SS at 1.5% NaCl (**Figures 9(b)** and **11(b)**) in the presence of ROSO compound remained generally the same even though there was significant improvement in the corrosion rate values from potentiodynamic polarization test, however there seems to be mild improvement for the
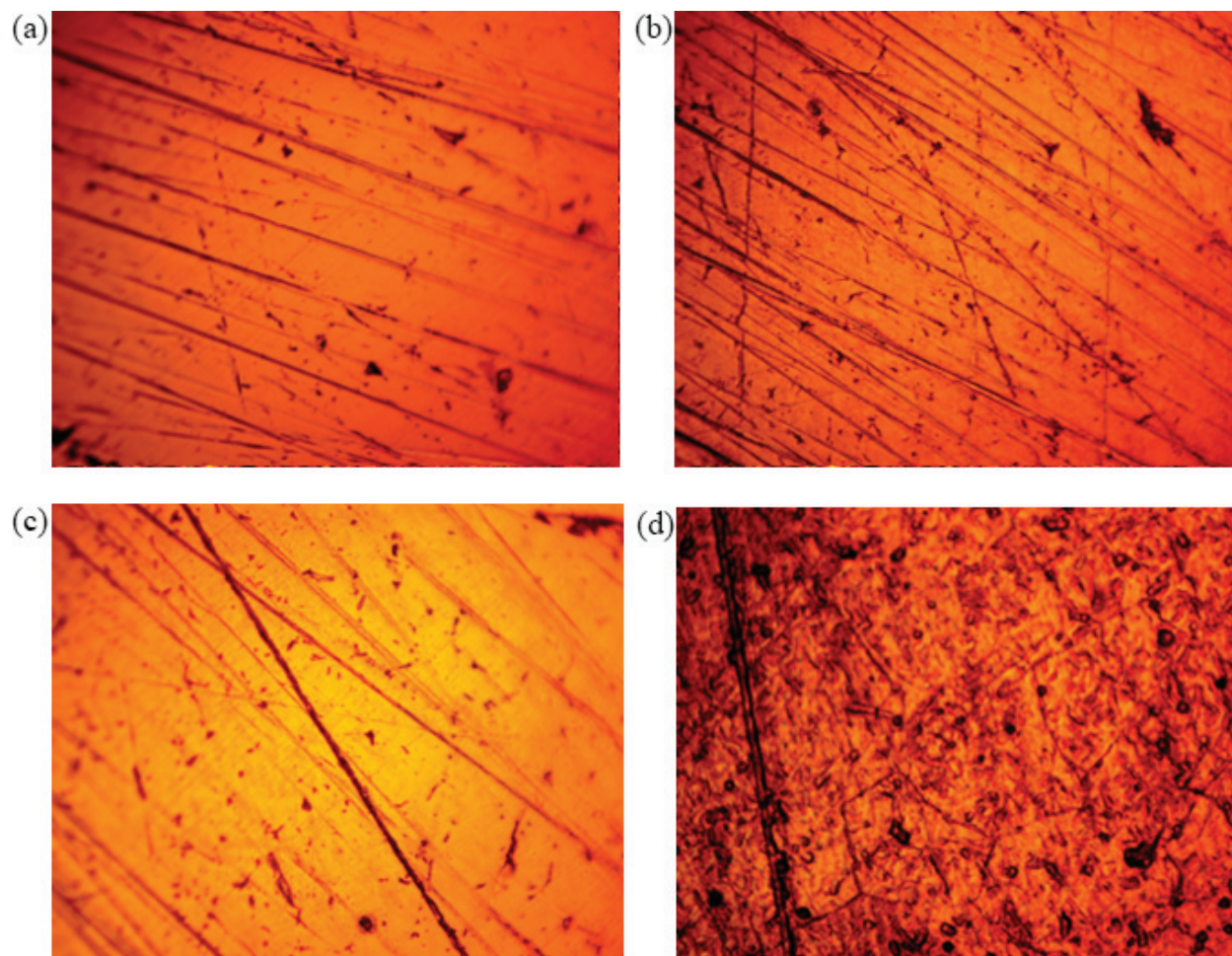
Figure 8. Optical microscopy image 316SS at mag. 40× (a) before corrosion, (b) at 0% NaCl, (c) at 0.25% NaCl and (d) at 1.5% NaCl.
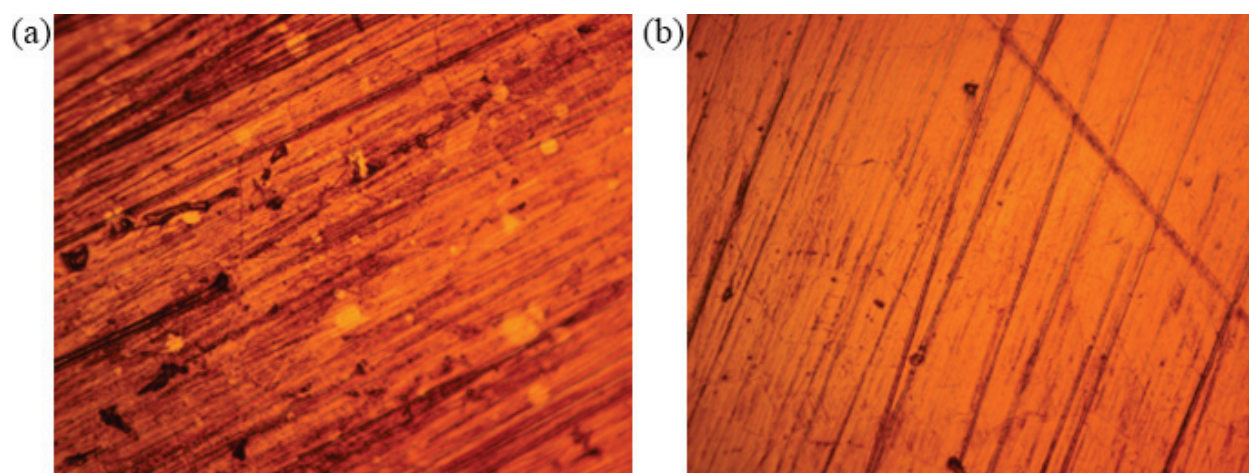

Figure 9. Optical microscopy image 301SS in the presence of ROSO compound (a) at 0.25% NaCl and (b) at 1.5% NaCl.
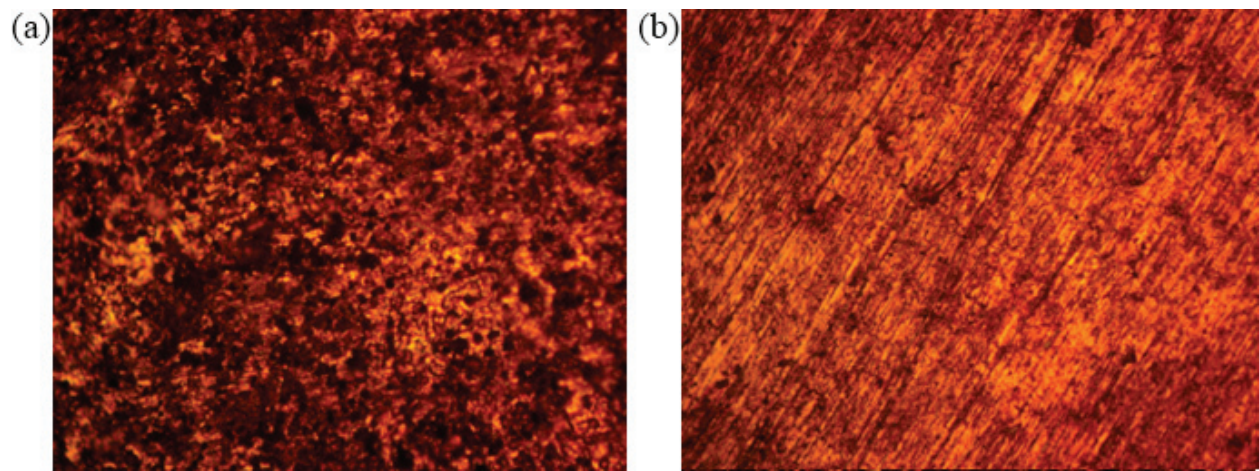
Figure 10. Optical microscopy image 304SS in the presence of ROSO compound (a) at 0.25% NaCl and (b) at 1.5% NaCl.
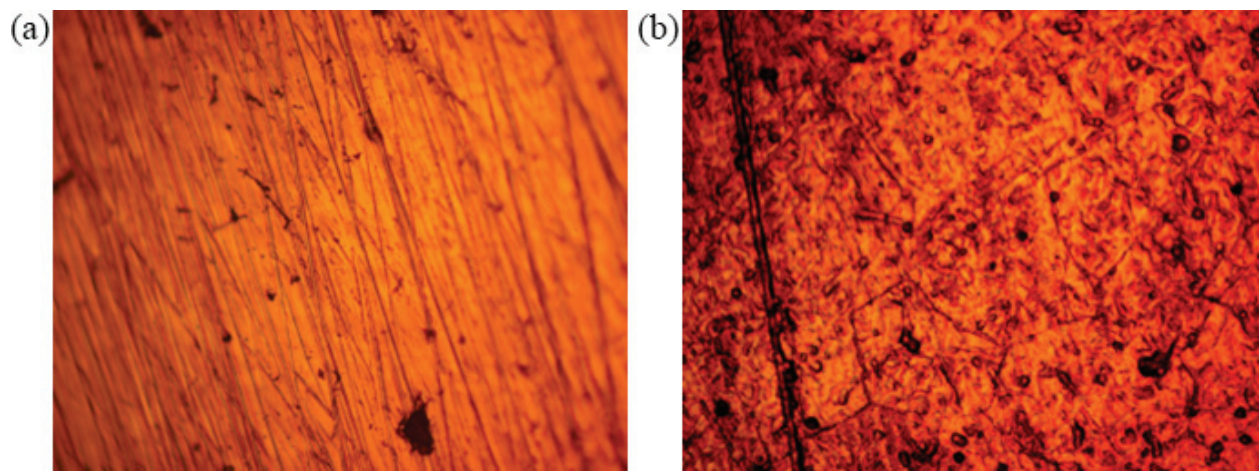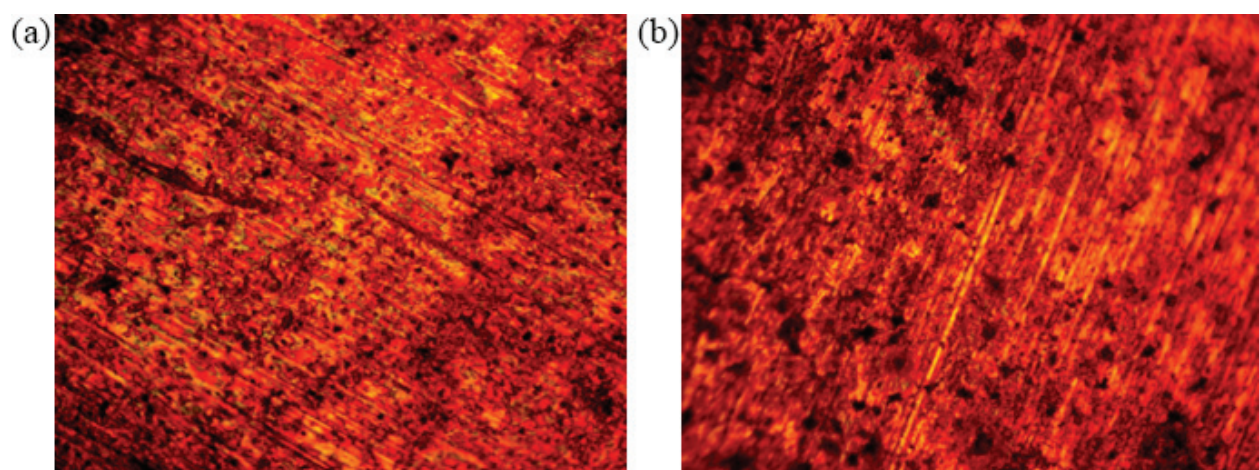

Figure 11. Optical microscopy image 316SS in the presence of ROSO compound (a) at 0.25% NaCl and (b) at 1.5% NaCl.

Figure 12. Optical microscopy image 304SS in the presence of ANL compound (a) at 0.25% NaCl and (b) at 1.5% NaCl.

images in Figures **9(a)** and **11(a)**. 304SS image (**Figure 10(a)**) showed significant increase in the number of micro-pits despite improvement in general corrosion rate value from the corrosion test. There appears to be smaller but more micro-pits compared to fewer but larger pits in **Figure 7(c)**, while **Figure 10(b)** showed no visible pits compared to **Figure 7(d)** in the presence of ROSO. Comparing the observation on 304SS with **Figure 12(a)** and (b), the optical images of 304SS from the corrosive solution in the presence of ANL compound are quite different from the images obtained in the presence of ROSO. There seems to be a remarkable improvement in the morphology of 304SS at 0.25%NaCl/ANL compared to 304SS at 0.25%NaCl/ROSO. The corrosion pits are significantly smaller and the steel surface is not as badly damaged like the surface from ROSO compound. Quite the contrary observation was obtained for 304SS at 1.5% NaCl/ANL compared to 304SS at 1.5%NaCl/ROSO. These observations show that chemical compounds are specific in action during corrosion inhibition.

3. Conclusion

Chloride concentration in 2 M H_2SO_4 had strong electrochemical effect on the pitting corrosion resistance and passivation behavior 301SS, 304SS and 316SS. 316SS showed the highest pitting corrosion resistance with resilient passivation behavior while 304SS failed immediately after anodic polarization in the presence of chlorides. The corrosion rates of the stainless steels generally increased with increase in chloride concentration. ROSO compound significantly reduced the corrosion rates of the stainless steels studied with notable improvement in their potentiodynamic polarization and passivation behavior; however it had detrimental effect on the pitting susceptibility of 304SS at lower chloride concentrations. ANL compound further reduced the corrosion rates of the stainless steels with particular improvement in morphology of 304SS but no changes in the potentiodynamic polarization and passivation behavior of 304SS was observed, hence limited pitting corrosion inhibition.

Acknowledgements

Author details

Roland Tolulope Loto

Address all correspondence to: tolu.loto@gmail.com

Department of Mechanical Engineering, Covenant University, Ota, Ogun State, Nigeria

References

[1] Alves H, Agarwal DC, Werner H. Nace–International Corrosion Conference Series; 2006, Houston, Texas.

[2] Pardo A, Merino MC, Coy AE, Viejo F, Arrabal R, Matykina E. Effect of Mo and Mn additions on the corrosion behaviour of AISI 304 and 316 stainless steels in H_2SO_4. Corrosion Science. 2008;**50**(3):780-794. DOI: 10.1016/j.corsci.2007.11.004

[3] Refaey SAM, Taha F, Abd El-Malak AM. Corrosion and inhibition of 316L stainless steel in neutral medium by 2-mercaptobenzimidazole. International Journal of Electrochemical Science. 2006;**1**:80-91

[4] Williams DE, Westcott C, Fleischmann M. Stochastic models of pitting corrosion of stainless steels. II. Measurement and interpretation of data at constant potential. Journal of the Electrochemical Society. 1985;**132**:1796-1804. DOI: 10.1149/1.2114221

[5] Shibata T, Takeyama T. Pitting corrosion as a stochastic process. Nature. 1976;**260**:315-316. DOI: 10.1038/260315a0

[6] Szklarska-Smialowska Z. Progress in understanding pitting corrosion. Electrochemical Society Proceedings. 2002;**13**:251-265

[7] Soltis J. Passivity breakdown, pit initiation and propagation of pits in metallic materials. Corrosion Science. 2015;**90**:5-22. DOI: 10.1016/j.corsci.2014.10.006.

[8] Newman RC, Foong TM, Sieradzki K. Validation of a percolation model for passivation of Fe.Cr alloys: I current efficiency in the incompletely passivated state. Corrosion Science. 1988;**28**(5):523–527. DOI: 10.1016/0010-938X(88)90074-1

[9] Song Q, Newman RC, Cottis RA, Sieradzki K. Validation of a percolation model for passivation of Fe–Cr alloys: Two-dimensional computer simulations. Journal of the Electrochemical Society. 1990;**137**:435-439. DOI: 10.1149/1.2086458

[10] Song Q, Newman RC, Cottis RA, Sieradzki K. Computer simulation of alloy passivation and activation. Corrosion Science. 1990;**31**:621–626. DOI: 10.1016/0010-938X(90)90171-Z

[11] Burstein GT, Marshall PI. The coupled kinetics of film growth and dissolution of stainless steel repassivating in acid solutions. Corrosion Science. 1984;**24**(5):449–462. DOI: 10.1016/0010-938X(84)90070-2

[12] Uhlig HH. The absorption theory of passivity and the flade potential. Zeitscrift für Elektrochemie. 1958;**62**(6–7):626-632

[13] Macdonald DD. The point defect model for the passive state. Journal of the Electrochemical Society. 1992;**139**(12):3434-3449

[14] Ahn SJ, Won HSK, Macdonald DD. Role of chloride ion in passivity breakdown on iron and nickel. Journal of the Electrochemical Society. 2005;**152**(11):B482-B490. DOI: 10.1149/1.2048247

[15] Kazuhiro Teramoto K, Asami K, Hashimoto K. The composition of passive films on ferritic 30 Cr stainless steels in H_2SO_4. Boshoku Gijutsu. 1978;**27**:57-61

[16] Hoar T, Mears D, Rothwell G. The relationships between anodic passivity, brightening and pitting. Corrosion Science. 1965;**5**(4):279-289. DOI: 10.1016/S0010-938X(65)90614-1

[17] Streicher MA. Pitting corrosion of 18Cr-8Ni stainless steel. 1956;**103**(7):375–390. DOI: 10.1149/1.2430359

[18] Matsuda S, Uhlig H. Effect of pH, sulfates, and chlorides on behavior of sodium chromate and nitrite as passivators for steel. Journal of the Electrochemical Society. 1964;**111**(2):156-161

[19] Uhlig HH, Lord SS Jr. Amount of oxygen on the surface of passive stainless steel. Journal of the Electrochemical Society. 1953;**100**(5):216-221. DOI: 10.1149/1.2781107

[20] Kolotyrkin JM. Effects of anions on the dissolution kinetics of metals. Journal of the Electrochemical Society. 1961;**108**(3):209-216. DOI: 10.1149/1.2428048

[21] Eklund GS. The effect of additives on the reaction mechanism of the $Pb/PbSO_4$ electrode. Journal of the Electrochemical Society. 1974;**121**(4):467-473. DOI: 10.1149/1.2401839

[22] Pistorius PC, Burstein GT. Metastable pitting corrosion of stainless steel and the transition to stability. Philosophical Transactions of the Royal Society A. 1992;**341**:531-542. DOI: 10.1098/rsta.1992.0114

[23] Burstein GT, Mattin SP. Repetitive nucleation of corrosion pits on stainless steel and the effects of surface roughness. Journal of the Electrochemical Society. 2001;**148**(12): B504-B516. DOI: 10.1149/1.1416503

[24] Frankel GS. Pitting corrosion of metals a review of the critical factors. Journal of the Electrochemical Society. 1998;**145**(6):2186-2198

[25] Pride ST, Scully JR, Hudson JL. Metastable pitting of aluminum and criteria for the transition to stable pit growth. Journal of the Electrochemical Society. 1994;**141**(11):3028-3040. DOI: 10.1149/1.2059275

[26] Laycock NJ, Newman RC. Localised dissolution kinetics, salt films and pitting potentials. Corrosion Science. 1997;**39**(10–11):1771-1790. DOI: 10.1016/S0010-938X(97)00049-8

[27] Suter T, Webb E, Böhni H, Alkire RC. Pit initiation on stainless steels in 1 M NaCl with and without mechanical stress. Journal of the Electrochemical Society. 2001;**148**(5):B174-B185. DOI: 10.1149/1.2059275

[28] Pistorius PC, Burstein GT. Aspects of the effects of electrolyte composition on the occurence of metastable pitting on stainless steel. Corrosion Science. 1994;**36**:525-538. DOI: 10.1016/0010-938X(94)90041-8

[29] Burstein GT, Mattin SP. Nucleation of corrosion pits on stainless steel. Philosophical Magazine Letters. 1992;**66**(1–4):127-131. DOI: 10.1016/0010-938X(93)90133-2

[30] Burstein GT, Pistorius PC, Mattin SP. The nucleation and growth of corrosion pits on stainless steel. Corrosion Science. 1993;**35**(1–4):57-62. DOI: 10.1016/0010-938X(93)90133-2

[31] Williams DE, Stewart J, Balkwill PH. The nucleation, growth and stability of micropits in stainless steel. Corrosion Science. 1994;**36**(7):1213-1235. DOI: 10.1016/0010-938X(94)90145-7

[32] Virtanen S, Kobayashi Y, Böhni H. In: Kelly RG, Frankel GS, Natishan PM, Newman RC, editors. Critical Factors in Localized Corrosion III. Pennington: Electrochemical Society; 1999. p. 281-290

[33] Ilevbare GO, Burstein GT. The role of alloyed molybdenum in the inhibition of pitting corrosion in stainless steels. Corrosion Science. 2001;**43**(3):485-513. DOI: 10.1016/S0010938 X(00)00086-X

[34] Wu J, Li X, Du C, Wang S, Song Y. Effects of Cl^- and SO_4^{2-} ions on corrosion behavior of X70 steel. Journal of Materials Science and Technology. 2005;**21**(1):28-32

[35] Ericson S, Kurol J. Inhibitive action of cannabis plant extract on the corrosion of copper in 0.5M H_2SO_4. International Journal of Electrochemical Science. 2013;**8**:5851-5865

[36] Cabral-Miramontes JA, Barceinas-Sánchez JDO, Poblano-Salas CA, Pedraza-Basulto GK, Nieves-Mendoza D, Zambrano Robledo PC, Almeraya-Calderón F, Chacón-Nava JG. Corrosion behavior of AISI 409Nb stainless steel manufactured by powder metallurgy exposed in H_2SO_4 and NaCl solutions. International Journal of Electrochemical Science. 2013;**8**:564-577

[37] Saadawy M. Effect of inorganic anions on the pitting behaviour of austenitic stainless steel 304 in H_2SO_4 solution containing chloride ion. International Journal of Electrochemical Science. 2016;**11**:2345-2359

[38] Loto RT. Pitting corrosion evaluation of austenitic stainless steel type 304 in acid chloride media. Journal of Materials and Environmental Science. 2013;**4**:448-459

[39] Yi Y, Cho P, Al Zaabi A, Addad Y, Jang C. Potentiodynamic polarization behaviour of AISI type 316 stainless steel in NaCl solution. Corrosion Science. 2013;**74**:92-97. DOI: 10.1016/j.corsci.2013.04.028

[40] Guan L, Zhang B, Yong XP, Wang JQ, Han EH, Ke W. Effects of cyclic stress on the metastable pitting characteristic for 304 stainless steel under potentiostatic polarization. Corrosion Science. 2015;**93**:80. DOI: 10.1016/j.corsci.2015.01.009

[41] Réguer S, Dillmann P, Mirambet F. Buried iron archaeological artefacts: Corrosion mechanisms related to the presence of Cl^- containing phases. Corrosion Science. 2007;**49**(6): 2726-2744. DOI: 10.1016/j.corsci.2006.11.009

[42] ASTM G1–03. Standard Practice for Preparing, Cleaning, and Evaluating Corrosion Test Specimens [Internet]. 2011. Available from: http://www.astm.org/Standards/G1 [Accessed: May 30, 2016].

[43] ASTM G59–97. Standard Test Method for Conducting Potentiodynamic Polarization Resistance Measurements [Internet]. 2014. http://www.astm.org/Standards/G31 [Accessed: May 30, 2016].

[44] ASTM G102–89. Standard Practice for Calculation of Corrosion Rates and Related Information from Electrochemical Measurements [Internet]. 2015. e1. http://www.astm.org/Standards/G31 [Accessed: May 30, 2016].

[45] Choi Y, Nesic S, Ling S. Effect of H_2S on the CO_2 corrosion of carbon steel in acidic solutions. Electrochimica Acta. 2011;**56**(4):1752-1760. DOI: 10.1016/j.electacta.2010.08.049

[46] Jensen WB. The Lewis Acid-Base Concepts. New York: John Wiley and Sons, Inc.; 1980. p. 112-336. DOI: 10.1002/nadc.19800281014

[47] Bockris JOM, Drazic D, Despic AR. The electrode kinetics of the deposition and dissolution of iron. Electrochimica Acta. 1961;**4**(2–4):325-361. DOI: 10.1016/0013-4686(61)80026-1

[48] Bockris JOM, Kita H. The temperature coefficients of electrode potentials: II. The second isothermal temperature coefficient. Journal of the Electrochemical Society. 1961;**108**(7): 676-685. DOI: 10.1149/1.2428187

[49] International Stainless Steel Forum [Internet]. http://www.worldstainless.org/Files/issf/non-image-files/PDF/TheStainlessSteelFamily.pdf. [Accessed: March 30, 2017].

[50] Metallurgy of Mo in Stainless Steel, International Molybdenum Association [Internet]. http://www.imoa.info/molybdenum-uses/molybdenum-grade-stainless-steels/metallurgy-of-molybdenum-in-stainless-steel.php. [Accessed: March 30, 2017].

[51] Hiramatsu N, Stott FH. The effects of molybdenum on the high-temperature oxidation resistance of thin foils of Fe–20Cr–5Al at very high temperatures. Oxidation of Metals. 2000;**53**(56):561-576. DOI: 10.1023/A:1004689211302

[52] Abreu CM, Cristobal MJ, Losada R, Novoa XR, Pena G, Perez MC. Comparative study of passive films of different stainless steels developed on alkaline medium. Electrochimica Acta. 2004;**49**(17–18):3049-3056. DOI: 10.1016/j.electacta.2004.01.064

[53] Montemor MF, Simoes A, Ferreira MGS, Da Cunha MB. The role of Mo in the chemical composition and semiconductive behaviour of oxide films formed on stainless steels. Corrosion Science. 1999;**41**(1):17-34. DOI: 10.1016/S0010-938X(98)00126-7

[54] Lu YC, Clayton CR. An XPS study of the passive and transpassive behavior of molybdenum in deaerated 0.1 M HCl. Corrosion Science. 1989;**29**(8):927-937. DOI: 10.1016/0010-938X(89)90085-1

[55] Vignal V, Olive JM, Desjardins D. Effect of molybdenum on passivity of stainless steels in chloride media using ex situ near field microscopy observations. Corrosion Science. 1999;**41**(5):869-884

[56] Olefjord I, Brox B, Jelvestam U. Surface composition of stainless steels during anodic dissolution and passivation studied by ESCA. Journal of the Electrochemical Society. 1985;**132**(12):2854-2861. DOI: 10.1149/1.2113683

[57] Schultze JW, Lohrengel MM, Ross D. Nucleation and growth of anodic oxide films. Electrochimica Acta. 1983;**28**(7):973-984

[58] Sedriks AJ. Corrosion of Stainless Steels. New York, NY: John Wiley and Sons; 1996

[59] Schmuki P, Virtanen S, Isaacs HS, Ryan MP, Davenport AJ, Bohni H, Stenberg T. Electrochemical behavior of Cr_2O_3/Fe_2O_3 artificial passive films studied by in situ XANES. Journal of the Electrochemical Society. 1998;**145**(3):791-801. DOI: 10.1149/1.1838347

[60] Newman RC. The dissolution and passivation kinetics of stainless alloys containing molybdenum—1. Coulometric studies of Fe.Cr and Fe.Cr.Mo alloys. Corrosion Science. 1985;**25**(5):331-339. DOI: 10.1016/0010-938X(85)90111-8

[61] Szklarska-Smialowska Z. Pitting Corrosion of Metals. Houston, TX: NACE; 1986. p. 430

[62] Horvath J, Uhlig HH. Critical potentials for pitting corrosion of Ni, Cr-Ni, Cr-Fe, and related stainless steels. Journal of the Electrochemical Society. 1968;**115**(8):791-795. DOI: 10.1149/1.2411433

[63] Ochao N, Moran F, Pebre N. The synergistic effect between phosphonocarboxylic acid salts and fatty amines for the corrosion protection of a carbon steel. Journal of Applied Electrochemistry. 2004;**34**(5):487-493

[64] Oguzie EE. Influence of halide ions on the inhibitive effect of congo red dye on the corrosion of mild steel in sulphuric acid solution. Materials Chemistry and Physics. 2004;**87**(1):212-217. DOI: 10.1016/j.matchemphys.2004.06.006

[65] Shalaby MN, Osman MM. Synergistic inhibition of anionic and nonionic surfactants on corrosion of mild steel in acidic solution. Anti-Corrosion Methods and Materials. 2001;**48**(5):309-318. DOI: 10.1108/EUM0000000005885

[66] Ebenso EE. Synergistic effect of halide ions on the corrosion inhibition of aluminium in H_2SO_4 using 2-acetylphenothiazine. Materials Chemistry and Physics. 2003;**79**(1):58-70. DOI: 10.1016/S0254-0584(02)00446-7

[67] Jayalakshmi M, Muralidharan VS. Correlation between structure and inhibition of organic compounds for acid corrosion of transition metals. Indian Journal of Chemical Technology. 1998;**5**:16-28

[68] Granese SL, Rosales BM, Oviedo C, Zebrino JO. The inhibition action of heterocyclic nitrogen organic compounds on Fe and steel in HCl media. Corrosion Science. 1992;**33**(9):1439-1453. DOI: 10.1016/0010-938X(92)90182-3

[69] Raicheva SN, Aleksiev BV, Sokolova EI. The effect of the chemical structure of some nitrogen- and sulphur-containing organic compounds on their corrosion inhibiting action. Corrosion Science. 1993;**34**(2):343-350. DOI: 10.1016/0010-938X(93)90011-5

[70] Abd El Rehim SS, Ibrahim MAM, Khaled KF. 4-Aminoantipyrine as an inhibitor of mild steel corrosion in HCl solution. Journal of Applied Electrochemistry. 1999;**29**(5):593-599

[71] Behpour M, Ghoreishi SM, Soltani N, Salavati-Niasari M, Hamadanian M, Gandomi A. Electrochemical and theoretical investigation on the corrosion inhibition of mild steel by

thiosalicylaldehyde derivatives in hydrochloric acid solution. Corrosion Science. 2008;**50**(8): 2172-2188. DOI: 10.1016/j.corsci.2008.06.020

[72] Loto RT, Oghenerukewe E. Inhibition studies of rosmarinus officinalis on the pitting corrosion resistance 439LL ferritic stainless steel in dilute sulphuric acid. Oriental Journal of Chemistry. 2016;**32**(5):2813-2832. DOI: 10.13005/ojc/320557

[73] Loto RT, Loto RO, Joseph OO, Akinwumi I. Electrochemical studies of the corrosion inhibition property of rosmarinus officinalis on mild steel in dilute sulphuric acid. Journal of Chemical and Pharmaceutical Research. 2015;**7**(7):105-116

[74] Bendahou M, Benabdellah M, Hammouti B. A study of rosemary oil as a green corrosion inhibitor for steel in 2M H_3PO_4. Pigment & Resin Technology. 2006;**35**(2):95-100. DOI: 10.1108/03699420610652386

[75] Susai RS, Mary R, Noreen A, Ramaraj R. Synergistic corrosion inhibition by the sodium dodecylsulphate–Zn^{2+} system. Corrosion Science. 2002;**44**(11):2243-2252. DOI: 10.1016/S0010-938X(02)00052-5

[76] Sahin M, Bilgiç S, Yılmaz H. The inhibition effects of some cyclic nitrogen compounds on the corrosion of the steel in NaCl mediums. Applied Surface Science. 2002;**195**(1–4):1-7. DOI: 10.1016/S0169-4332(01)00783-8

[77] Aharoni C, Ungarish M. Kinetics of activated chemisorption. Part 2. Theoretical models. Journal of the Chemical Society, Faraday Transactions. 1977;**73**:456-464

[78] Lowmunkhong P, Ungthararak D, Sutthivaiyakit P. Tryptamine as a corrosion inhibitor of mild steel in hydrochloric acid solution. Corrosion Science. 2010;**52**(1):30-36. DOI: 10.1016/j.corsci.2009.08.039

[79] Vračar LM, Dražić DM. Adsorption and corrosion inhibitive properties of some organic molecules on iron electrode in sulfuric acid. Corrosion Science. 2002;**44**(8):1669-1680. DOI: 10.1016/S0010-938X(01)00166-4